Study on Numerical Analysis Method for Electromagnetic Fluid Using Vector Finite Volume Method Consistent with Solenoidal Condition

Ryoji MURASHIGE, Akira YAMAGUCHI and Takashi TAKATA
Osaka University
2-1, Yamada, Suita, Osaka, Japan
murashige_r@qe.see.eng.osaka-u.ac.jp; yamaguchi@see.eng.osaka-u.ac.jp;
takata_t@see.eng.osaka-u.ac.jp

ABSTRACT

A multi-dimensional numerical method of electromagnetic fluid for finite volume method has been developed based on the Vector Finite Element Method (VFEM) that automatically satisfies the solenoidal condition, which means that a divergence of magnetic field should be zero, when it is achieved in an initial condition. The authors name it the Vector Finite Volume Method, VFVM.
In the VFVM, a magnetic flux density is defined at a center of computational cell surface. On the other hand, an electric field is defined at each side of the cell surface including boundary surfaces and is calculated using the velocity and the magnetic field.
In the present study, the authors propose a new modification method of electric field at the boundary cell with a comparative high computational efficiency and investigate its applicability based on some numerical examples. A parallel plate flow (Hartmann flow) is selected for the verification of the proposed method.

KEYWORDS

Computational fluid dynamics, Electromagnetic fluid, Vector finite volume method, Solenoidal condition

1. INTRODUCTION

Electromagnetic fluid such as liquid sodium is used as a coolant in fast-breeder reactor. In the fluid, the electric and magnetic field interact with each other and generate Lorentz force. It is possible to control the flow of the fluid by using the force. Hence, it is meaningful to depict the behavior of electromagnetic fluid under applied magnetic field. From this viewpoint, a numerical methodology is useful for investigating the fluid dynamics characteristics under an electromagnetic field.

In numerical analysis of electromagnetic fluid, emphasis should be placed on solving the induction equations consistent with the solenoidal condition. The solenoidal condition requires the divergence of the magnetic flux density to be zero at any point in space. Though it is required in physical viewpoint that the solenoidal condition stands, it is not simple and easy to satisfy its condition numerically. Many methods use iterative procedure so as to achieve the solenoidal condition, which results in the increase of the computational cost [1]. In order to enhance the computational efficiency, it is desirable to solve the induction equations without relying on an iterative procedure or with a less iterative manner.

The Vector Finite Element Method (VFEM) is the numerical technique that is able to solve the equations without iterations [2]. We apply this methodology to finite volume method (called the Vector Finite Volume Method, VFVM). The VFVM satisfies the solenoidal condition automatically. However, a consideration of electric field is required at boundary in this method.

In the present study, we have proposed a new method about the boundary condition of the electric field and carried out a benchmark analysis in order to investigate its applicability. We have analyzed a parallel plate flow under applied magnetic flux density (Hartmann flow). The computational results are compared with theoretical results and the original VFEM. After the verification of the applicability, we have also analyzed numerically a rectangular channel flow where a constant magnetic flux density is embedded partially.

2. NUMERICAL METHOD

2.1. Governing Equations

The governing equations of electromagnetic fluid are described as the coupling of the governing equations of fluid dynamics and electromagnetic field. The motion of the fluid is depicted by the follows:

$$\nabla \cdot \mathbf{u} = 0 \tag{1}$$

$$\frac{\partial \mathbf{u}}{\partial t} + \mathbf{u} \cdot \nabla \mathbf{u} = -\frac{1}{\rho}\nabla p + \nu \nabla^2 \mathbf{u} + \frac{\sigma}{\rho}(\mathbf{u} \times \mathbf{B} + \mathbf{E}) \times \mathbf{B} \tag{2}$$

$$\nabla \cdot \mathbf{B} = 0 \tag{3}$$

$$\mathbf{E} = -\mathbf{u} \times \mathbf{B} + \frac{1}{\sigma\mu}\nabla \times \mathbf{B} \tag{4}$$

$$\frac{\partial \mathbf{B}}{\partial t} = -\nabla \times \mathbf{E} \tag{5}$$

Here, **u**, **B**, **E** and p are velocity vector, magnetic flux density vector, electric field vector and pressure, respectively. ρ, ν, σ and μ are density, kinetic viscosity, electric conductivity and magnetic permeability. In this paper, a constant value of material properties is assumed for simplicity as well as no external force except the Lorentz force.

Equations (1) and (2) are the governing equations of fluid dynamics. They indicate the continuity of mass and momentum of fluid, respectively. The coupling of fluid dynamics and electromagnetic field is described as the third term on the right side of Eq.(2). It is the external force term expressed as the Lorentz force.

Equations (3), (4) and (5) are the governing equations of electromagnetic field. Equation (3) is named Gauss's law of magnetism and signifies the conservation law of magnetic field. It is also called the solenoidal condition. Equation (4) is obtained by the combination of Ohm's law and Ampere's law. Equation (5) is called Maxwell-Faraday equation and accounts for the relationship between a time-varying magnetic field and an induced electric field.

Many numerical techniques [3],[4] for electromagnetic fluid calculate the magnetic field using not Eqs.(3)-(5) but the following induction equation that is obtained by substituting

Eqs.(3) and (4) into Eq.(5).

$$\frac{\partial \mathbf{B}}{\partial \mathrm{t}} = \nabla \times (\mathbf{u} \times \mathbf{B}) + \frac{1}{\sigma \mu} \nabla^2 \mathbf{B} \tag{6}$$

It is apparent that the solenoidal condition (Eq.(3)) is not a sufficient condition but a necessary condition for Eq.(6). Therefore, an iterative procedure is required in the techniques that solve Eq.(6) so as to satisfy the solenoidal condition.

In the VFEM, Eqs.(4) and (5) are solved directly instead of the induction equation (Eq.(6)). The electric and magnetic flux density fields are defined separately in space so that one achieves solenoidal condition automatically. We have extended this methodology to a finite volume method.

2.2. Vector Finite Volume Method

Firstly, let us discuss the solenoidal condition using Eq.(5) mathematically. Adding the divergence operation to Eq.(5), one obtains the following equation.

$$\frac{\partial}{\partial \mathrm{t}} (\nabla \cdot \mathbf{B}) = -\nabla \cdot (\nabla \times \mathbf{E}) = 0 \tag{7}$$

As in Eq.(7), the solenoidal conodition will be satisfied automatically when it is achieved in an initial condition. This is the main feature of the VFVM same with the VFEM. Hence, the definition point of electric field is arranged so that the divergence of the rotation must be null numerically. Figure 1 shows the arrangement of discrete points. While the magnetic flux density is defined at the center of the cell surface, the electric field is defined at the side of the cell surface.

Fig. 1 Arrangement of Variables in the Flow Field and the Electromagnetic Field

The concept of practical discretization in the VFVM is shown in Fig. 2. In each control volume, the surface integral of the rotation of electric field at each surface is equivalent to the line integral of the boundary electric fields according to Stokes' theorem. In terms of the contiguous two faces (S_1 and S_2), they share one side (side *l*) and the directions of their line integrals are reversed each other. Therefore the value of line integration at the side *l* is negated. Considering the line integrals at all surfaces in the control volme, the value of any line integral of electric field is negated. Consequently, the summation of the surface integrals in a

whole control volume is exactly null in the present method.

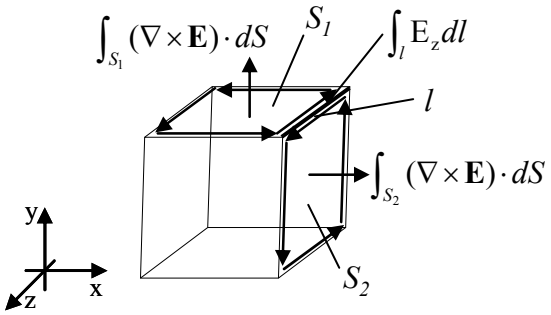

Fig. 2 Schematic Diagram of Vector Finite Volume Method

2.3. Consideration of Boundary Condition of Electric Field

It can be said that the VFVM is an efficient numerical technique for reducing computational cost. However, one should consider the appropriate electric field at boundary, which is consistent with the boundary condition of the magnetic flux density in the VFVM. It is noted that the boundary condition of electric field will be included in the discretized equation in a finite element method. Therefore, no consideration of the electric field boundary condition is necessary in the VFEM. Some problems will occur in VFVM if no consistency between the electric field and magnetic flux density at boundary is applied. Furthermore, the consistency between the boundary surface and the computational cell will be also of importance. It is also noted that the consideration of the boundary condition of the electric field does not come from the material characteristics at the boundary but come from the boundary condition of the magnetic flux density given in the numerical simulation.

One of the simplest way is to give the electric field as zero (in this paper, we say “No modification”). However, this might lead unrealistic magenetic flux density even though the solenoidal condition is satisfied because no consistency between the boundary surface and the computational cell is applied. The other one calculates the electric field at boundary using the virtual cell concept and the boundary condition of magnetic flux denstiy. This method does not lead unrealistic magnetic flux density. However, the magnetic flux density at boundary obtained from this method will not satisfy a constant magnetic flux density because of $\nabla\times\mathbf{E}\neq\mathbf{0}$. Hence when the constant magnetic flux density is applied at the boundary, the solenoidal condition will not be satisfied. In the present study, a new method is proposed to eliminate these problems.

In the proposed method, the electric field at boundary is expressed using a predictor and a corrector. Firstly, the predictor is calculated using the virtual cell concept and the magnetic flux density at boundary by solving Eq.(4). Then the corrector is introduced in case of a constant magnetic flux density condition so that the following equation should be satisfied.

$$\nabla\times\mathbf{E}=0 \quad \text{(at boundary)} \tag{8}$$

In this paper, the corrector (δE) is introduced at each cell as shown in Fig. 3. Since each side is shared by two cells, the electric field defined at the side is revised by two adjoining correctors. For example, the electric field E_c defined at the side C is revised as follows (see

Fig. 3):

$$E_C = E_C^* + (\delta E_{right} - \delta E_{left}) \tag{9}$$

where δE_c^*, δE_{left} and δE_{right} are the predictor and the correctors at cell left and right, respectively.

Substituting Eq.(9) into (8) at all boundary region where a constant magnetic flux density is given, one obtains the system of equation for the corrector. In the present study, the corrector δE is calculated by Bi-Conjugate Gradient Stabilized (BiCGS) method.

The present method corrects the electric field only at boundary surfaces, while the iterative procedure method, based on Eq.(6) [3],[4], performes the correction of the magnetic field at all computational cells. Hence this method has an advantage to enhance the computational efficiency comparing with the iterative procedure. It is said that the corrector acts like an external force that keeps the magnetic flux density constant at the boundary.

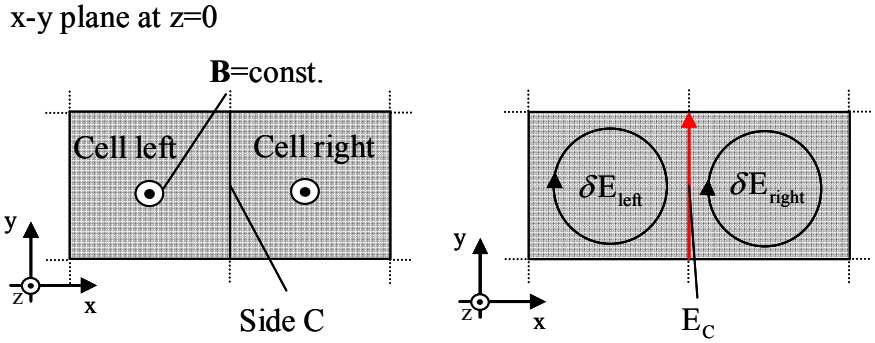

Fig. 3 Manner of Giving the Corrector of Electric Field at Boundary

2.4. Computational Method

In the present study, a finite difference with a structural mesh arrangement in Cartesian coordinates is applied. With regard to the order of the differential scheme, a second order central difference is applied in a diffusion term, and a first order upwind difference scheme is applied in a convection term. In the analysis of the flow field, the Simplified Marker And Cell (SMAC) method is used [5]. With regard to electromagnetic fields, the Lorentz force term in Eq.(2) and Eqs.(4) and (5) are discretized explicitly. The discretizations of the governing equations are shown as follows:

$$\nabla \cdot \mathbf{u}^{n+1} = 0 \tag{11}$$

$$\frac{\mathbf{u}^{n+1} - \mathbf{u}^n}{\Delta t} + \mathbf{u}^n \cdot \nabla \mathbf{u}^n = -\frac{1}{\rho}\nabla p^{n+1} + \nu \nabla^2 \mathbf{u}^n + \frac{\sigma}{\rho}\left(\mathbf{u}^n \times \mathbf{B}^n + \mathbf{E}\right) \times \mathbf{B}^n \tag{12}$$

$$\mathbf{E} = -\mathbf{u}^{n+1} \times \mathbf{B}^n + \frac{1}{\sigma\mu}\nabla \times \mathbf{B}^n \tag{13}$$

$$\frac{\mathbf{B}^{n+1} - \mathbf{B}^n}{\Delta t} = -\nabla \times \mathbf{E} \tag{14}$$

where superscript n and n+1 are the current and subsequent time step, respectively. The solenoidal condition is satisfied automatically in the VFVM. So the discretization of Eq.(3) is not necessary. Figure 4 shows the flow chart of the calculation.

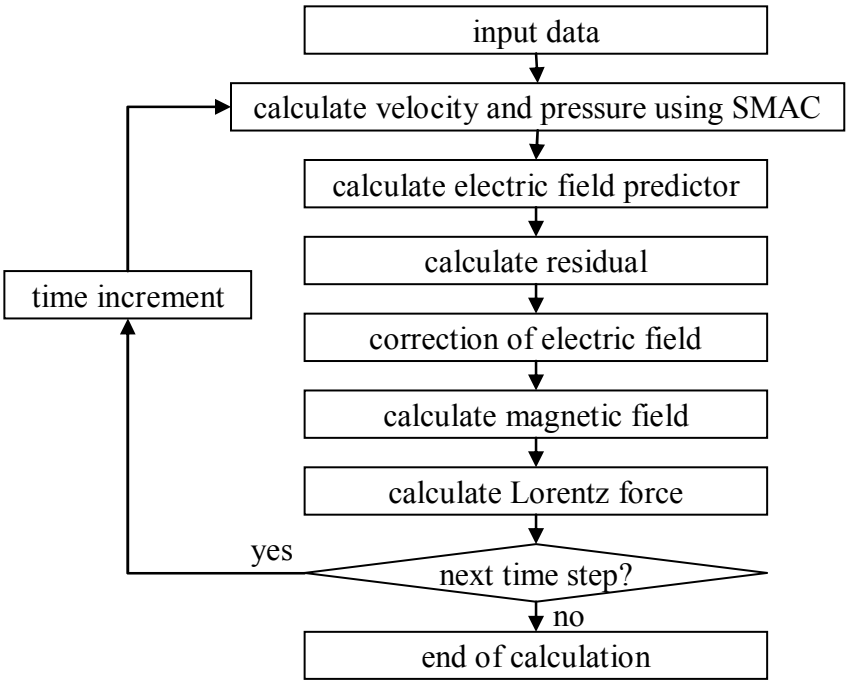

Fig. 4 Flow Chart of the Calculation

3. BENCHMARK ANALYSES

3.1. Parallel Plate Flow Analysis

In order to investigate the applicability of the present method, a parallel plate flow under applying constant magnetic flux density is analyzed numerically. This flow is called Hartmann flow and theoretical flow profile is given the following eqution [6].

$$u(y) = \frac{Ha}{\tanh(Ha) - Ha}\left(\frac{\cosh(Ha \cdot y)}{\cosh(Ha)} - 1\right) \tag{15}$$

Here, u is the velocity component in the main flow direction and Ha is the Hartmann number and is obtained as:

$$Ha = \sqrt{\frac{\sigma}{\rho\nu}} B_0 L \tag{16}$$

where, B_0 is the magnitude of applied magnetic flux density, and L is the half distance between two flat plates. Analytical result of the VFVM using the new method is compared with the “No modification” method (in which electric field is defined as zero at boundary), the original VFEM [2] and the theoretical result.

3.1.1. Analytical model

The analytical model is shown in Fig. 5. The size of analytical region is 10×2.0×20[m]. The free-slip condition is applied in the x-y planes at z=0 and 20[m], and the non-slip condition is applied in the x-z planes at y=0 and 2.0[m]. Inlet velocity is given as the parabolic distribution that the average velocity is 1.0[m/s] and outlet condition is given as a constant pressure condition (P_B=0[Pa]). In terms of magnetic flux density, constant magnetic flux density (B_y=1.0[T]) is applied vertically at each parallel plate (y=0 and 2.0[m]). The electric conductivity of these parallel plates are same as that of the working fluid. In other boundary, magnetic flux density is continuous to the normal direction of the boundary. Because of this, the rotation of magnetic flux density is zero on the inlet and outlet planes at initial condition. A uniform magnetic flux density (**B** = (0.0, 1.0, 0.0)) is given in a whole analytic region as an initial condition in order to satisfy the solenoidal condition at the beginning of computation.

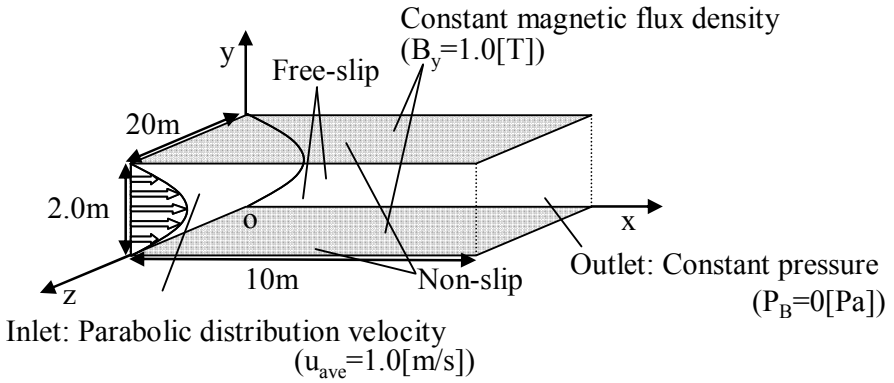

Fig. 5 Analytical Model of Hartmann Flow

Table 1 shows the analytical conditions. The analytical region is devided into 20×20×5 equally. In Table 1, Δt, t_{end}, ε_p and ε_E are the time increment, calculation time, the convergence criteria for pressure and electric field at boundary, respectively. Fluid is a virtual one and its properties are shown in Table 2.

Table 1. Analytical Conditions

Parameter	**Size** [m]	**Mesh**	Δt [s]	t_{end} [s]	ε_p	ε_E
Value	10×2.0×20	20×20×5	4.0×10^{-3}	2.0	1.0×10^{-10}	1.0×10^{-10}

Table 2. Fluid Properties

Property	ρ [kg/m^3]	ν [m^2/s]	σ [S/m]	μ [H/m]
Value	1.0	0.1	10	0.1

3.1.2. Results and discussions

Figure 6 shows the analysis results of present method of (a) velocity vectors and (b) Lorentz force vectors at z=10 [m]. As seen in Fig. 6, Lorentz force vectors near wall point to outlet

and near center point to inlet direction. By these forces, the fluid near wall is accelerated and near center is deaccelerated, that flatten the velocity profiles in y direction. Also, it is confirmed that the effect by Lorentz foece is notable near inlet area. Therefore the velocities form Hartmann flow profiles immediately in the analysis.

In order to investigate the applicability of the present method, velocity and magnetic profiles are compared with the theoretical result and other numerical results. Figures 7 and 8 show the comparison of the mainsteam velocity and the magnetic flux density profiles at the center (see right side of Fig.7), respectively.

Even though "No modification" agrees well with the theoretical reluts in terms of velocity profile, the magnetic flux density profiles are far different from the original VFEM ("VFEM" in Fig. 8). This is attributed to the boundary electric field. On the other hand, numerical results of the present method ("Present" in Figs. 7 and 8) are in good agreement with theoretical results and the VFEM in terms of both velocity and magnetic flux density profiles. This indicates the new method modifies the electric field successfully at the boundary.

Figure 9 shows the comparison of (a) induced electric field of z component and (b) Lorentz force of x component at the center of analytical region, respectively. In Fig. 9 (a), while electric field in negative direction is generated in present method, no modification obtains null electric field. Although the profiles of magnetic flux density are different between the present and no modification methods, little difference appears in the velocity profiles as in Fig. 7. Since the profile of the Lorentz force is just shifted in the no modification case, the similar velocity profile is achieved. Therefore, a large pressure gradient arises in the no modification method as shown in Fig. 10.

By these results, it is recognized that the proposed method is available for analysis of magnetohydrodynamic flow using the VFVM.

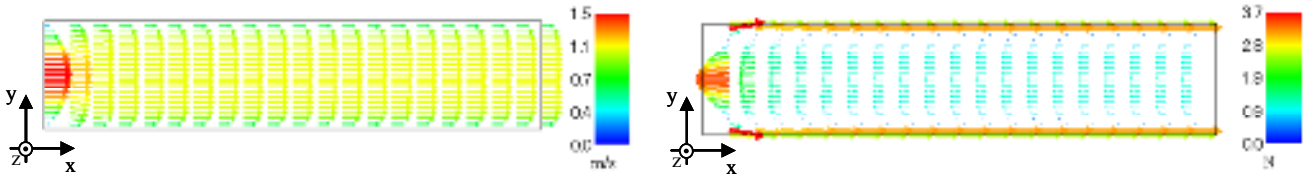

(a) Velocity vectors **(b) Lorentz force vectors**

Fig. 6 Analytical Results at z=10[m] (Present Method)

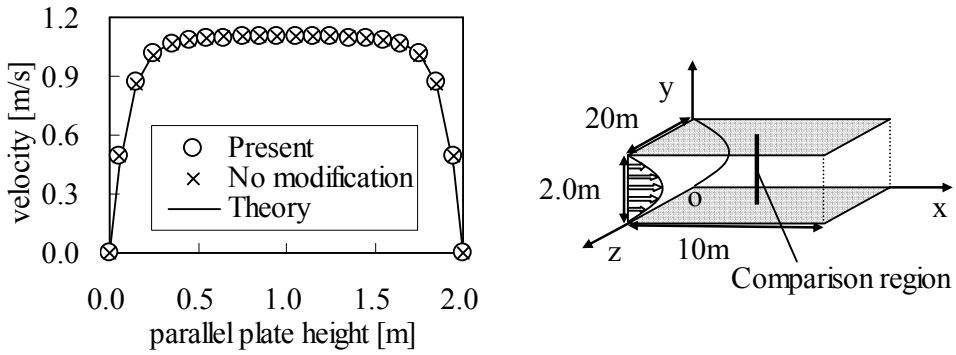

Fig. 7 Comparison of Mainstream Velocity Profiles at x=5.0, z=10[m]

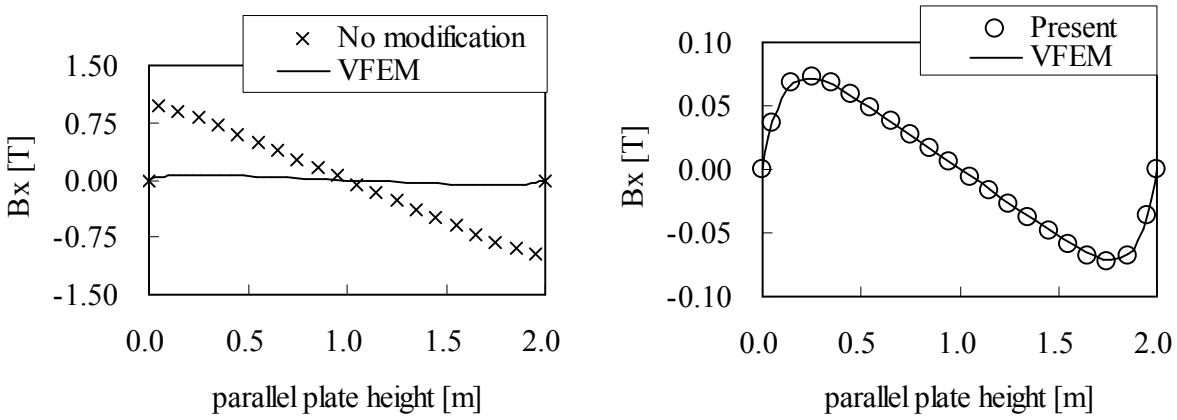

(a) No modification **(b) Present method**

Fig. 8 Comparison of Magnetic Flux Density Profiles at x=5.0, z=10[m]

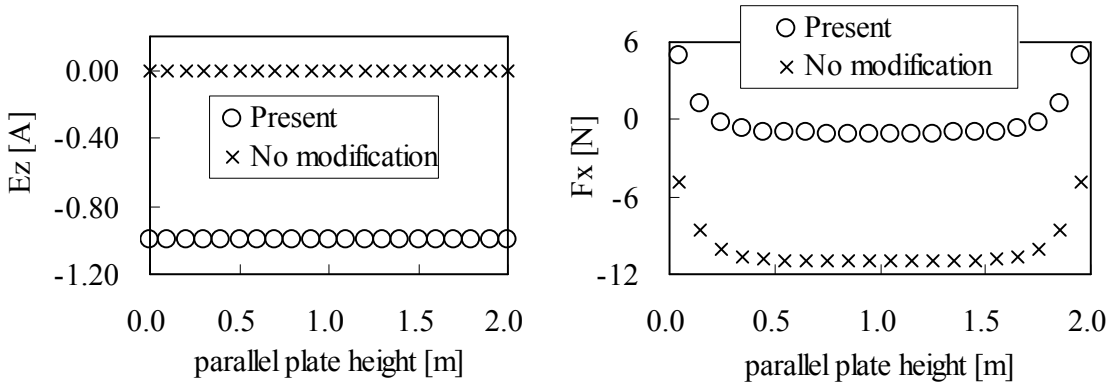

(a) Induced electric field **(b) Lorentz force**

Fig.9 Comparison of Profiles at x=5.0, z=10[m]

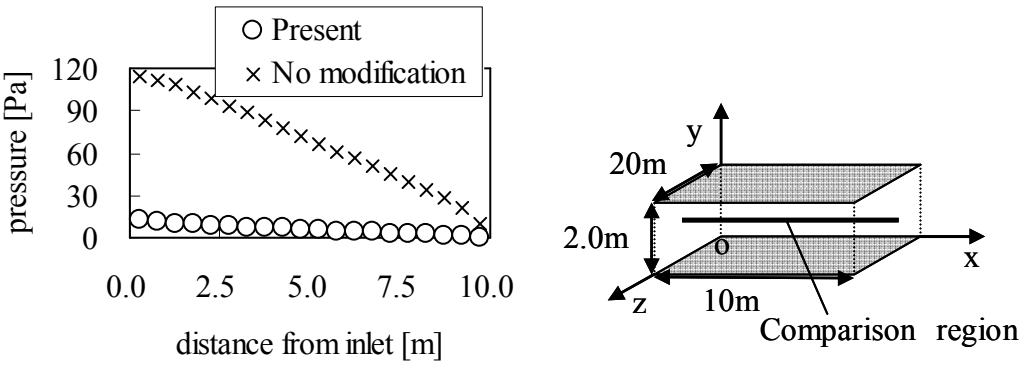

Fig. 10 Comparison of Pressure Profiles at y=1.05, z=10[m]

3.2. Rectangular Channel Flow Analysis

3.2.1. Analytical model

Fig. 11 shows the analytical region of rectangular channel flow. The size of the region is 20×2.0×10[m] and divided into 20×20×10 equally. The non-slip condition is applied both in the x-y plane and x-z plane. Uniform velocity (1.0[m/s]) is given in inlet. Outlet condition is constant pressure condition. In terms of the boundary condition of magnetic flux density, a uniform and constant value of 1.0[T] is applied only from x=4.0 to 14.0[m] in x-z planes at y=0 and 2.0[m]. In the other walls, including the x-y planes at z=0, 10[m] and the y-z planes at x=0, 20[m], a constant magnetic flux density of 0[T] is applied. The initial condition of magnetic flux density is a uniform (**B** = (0.0, 1.0, 0.0)) in applied magnetic flux density region (from x=4.0 to 14.0[m]) and the other region is given as zero. Table 3 shows the analytical parameters. As concerns a working fluid, the same fluid with Sec.3.1 is used.

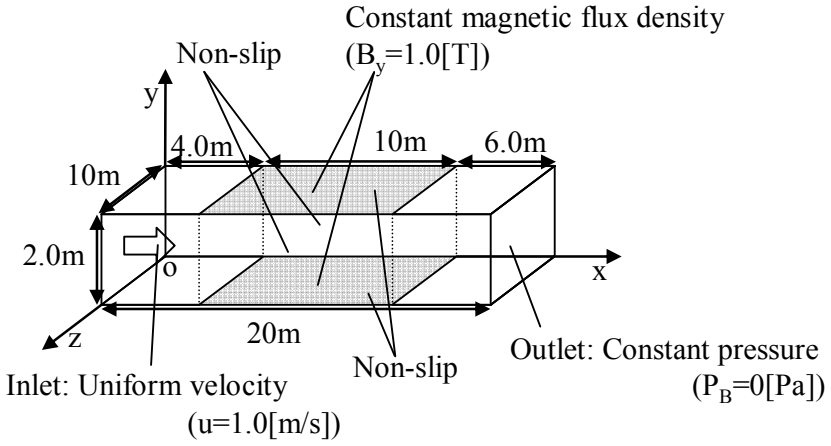

Fig. 11 Analytical Model of Rectangular Channel Flow

Table 3. Analytical Conditions

Parameter	Size [m]	Mesh	Δt [s]	t_{end} [s]	ε_p	ε_E
Value	20×2.0×10	20×20×10	4.0×10^{-3}	8.5	1.0×10^{-10}	1.0×10^{-10}

3.2.2. Results and discussions

The comparison of the cross-sectional velocity distribution at the center of the duct (z=5.0[m]) is indicated in Fig. 12. In case of the present method, a multi dimensional effect is investigated both at the inlet and the outlet of the magnetic field area caused by the side wall of the duct. On the contrary, the velocity profile is changed immediately in case of no modification method. Figure 13 shows the velocity pforile at the center. In both cases, the velocity profiles agree with that of the Hartmann flow at that region.

Figure 14 shows the distributions of (a) Lorentz force and (b) the pressure at the duct center along the main flow direction. As seen in Fig. 14, the higher Lorentz force and pressure

gradient are analyzed in the no modification method comparing with that in the proposed method. Thus, the immediate change of the velocity profile and almost no multi dimensional effect are investigated in the no modification case.

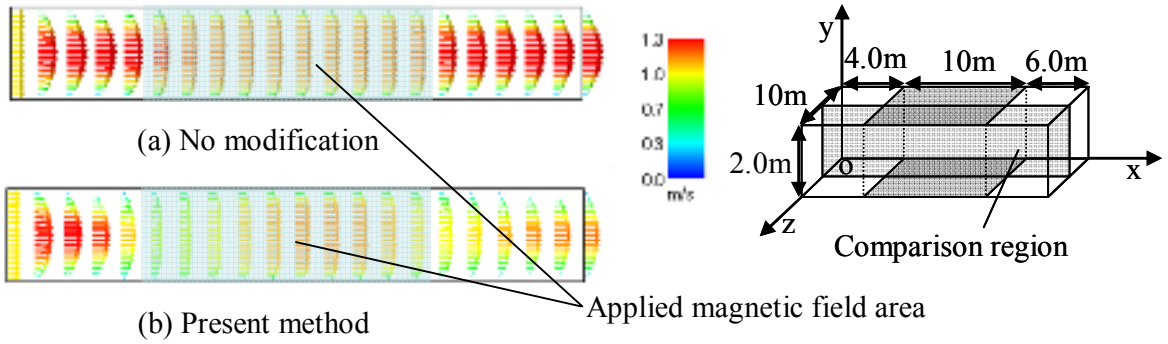

Fig. 12 Velocity Vectors at z=5.0[m]

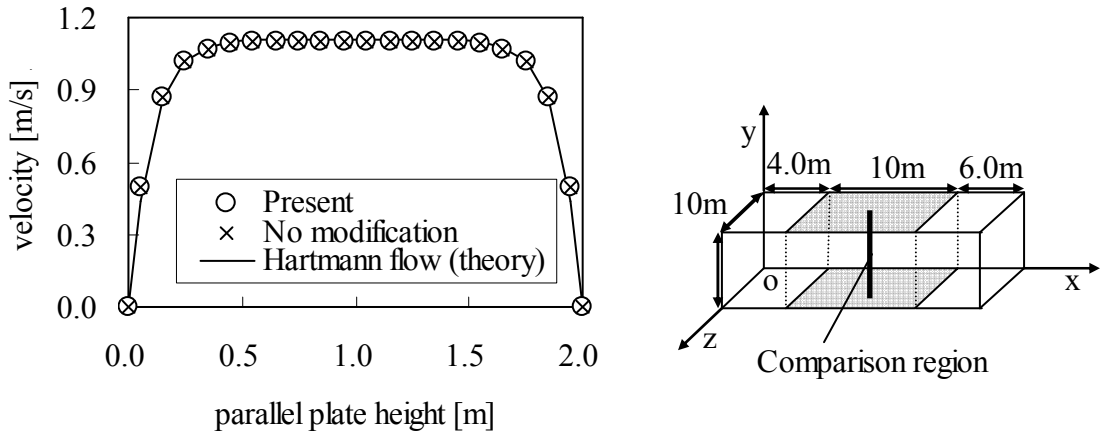

Fig. 13 Velocity Profiles at x=10, z=5.0[m] in Rectangular Flow

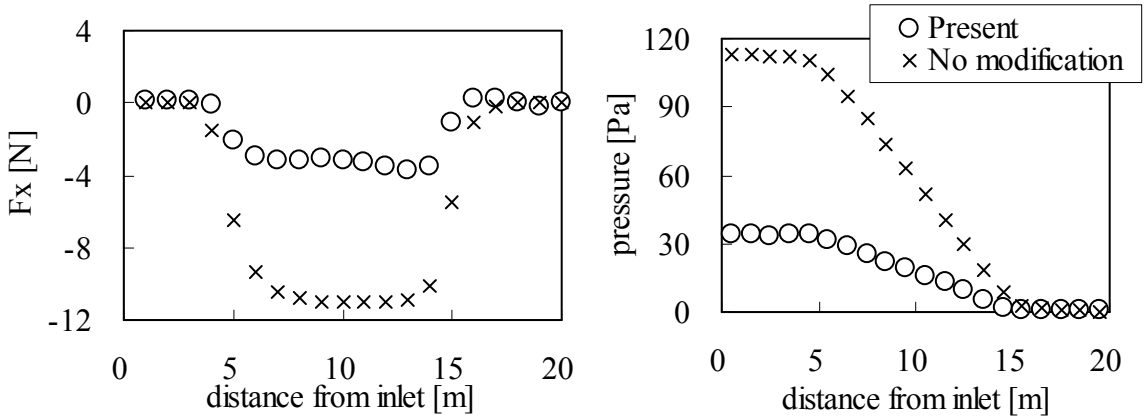

(a) Lorentz force **(b) pressure**

Fig. 14 Comparison of profiles at y=1.05, z=5.0[m]

From the benchmark result mentioned in Sec. 3.1, the present method seems to be applicable in a numerical analysis of thermo-electrically conducting fluid. However, it is noted that a mature consideration of the proposed method will be necessary in case of, such as, a boundary cell with high aspect ratio and a discontinuous magnetic flux density distribution.

4. CONCLUSIONS

In the present paper, the authors have extended the Vector Finite Element Method (VFEM) to finite volume method (VFVM) and proposed a new method of defining the electric field at boundary. In the proposed method, the electric field is calculated based on the Ohm's law and Ampere's law as a predictor. Then the corrector is introduced so as to satisfy consistency with the boundary condition of magnetic flux density. As a result of the benchmark analyses, the following conclusions are obtained.

In the no modification method where the electric field is set to zero at the boundary, even though the velocity profile agrees well with that in Hartmann flow, the magnetic flux density profile is far different from the original VFEM. It is confirmed that a consideration of the boundary electric field should be needed.

Since both the velocity and the magnetic flux density profiles are in good agreement with the theoretical result and the original VFEM in the parallel plate flow analysis, the proposed method is available for magnetohydrodynamic flow analysis.

In the present method, the iterative procedure is required only at the boundary surfaces in order to satisfy the solenoidal condition. The size of system equation becomes smaller than that of a cell based procedure such as solving the induction equation of magnetic field iteratively. Consequently, a high computational efficiency could be achieved.

In the future work, a mature investigation of the present method is planned when high aspect ratio of computational mesh is arranged and a discontinuous distribution of the magnetic flux density is assigned at boundary.

REFERENCES

[1] M. Matsumoto and T. Tanahashi, "Numerical Analysis of Thermo-electrically Conducting Fluids in a Cubic Cavity Using Vector Finite Element Method for Induction Equations," *ISIJ International*, Vol.43, No.6 pp.932-941, (2003)
[2] M. Matsumoto and T. Tanahashi, "Numerical analysis of the flow in the liquid metal by the vector finite element method, (in Japanese)" *15th Sym. on computational fluid dynamics B.*, **04-1**,(2001)
[3] Y. Oki and T. Tanahashi, "Numerical Analysis of Natural Convection of Thermo-Electrically Conducting Fluids in a Square Cavity under a Constant Magnetic Field (1st report)," *JSME INT. B.*, **59-562**, pp.1835-1842 (1993)
[4] T. Nakai and T. Tanahashi, "Numerical Analysis of Natural Convection of Thermo-Electrically Conducting Fluids in a Square Cavity under a Constant Magnetic Field (2nd report)," JSME INT. B., **63-605**, pp.201-208 (1997)
[5] M. Hirano, *Numerical Calculation and Visualization of Fluid Flow, 2nd Ed.,* Maruzen Publishing Co., Ltd, Tokyo & Japan (2004)
[6] Y. Oki and T. Tanahashi, "Entrance Flows of Electrically Conducting Fluids between Two Parallel Plates (Transient and Steady Flows)," *JSME Int. B.*, **58-545**, pp.14-21 (1991)